International Journal of Engineering & Applied Sciences (IJEAS)

Vol.7, Issue 3(2015)1-15

FREE VIBRATION ANALYSIS OF EDGE CRACKED FUNCTIONALLY GRADED BEAMS RESTING ON WINKLER-PASTERNAK FOUNDATION

Şeref Doğuşcan Akbaş

Assoc. Prof. Dr., E-mail: serefda@yahoo.com
Department of Civil Engineering, Bursa Technical University, Bursa, Turkey

Abstract

In this study, free vibration analysis of an edge cracked functionally graded cantilever beam resting on Winkler-Pasternak foundation. Material properties of the beam change in the thickness direction according to exponential distributions. The differential equations of motion are obtained by using Hamilton's principle. The considered problem is investigated within the Euler-Bernoulli beam theory by using finite element method. The cracked beam is modeled as an assembly of two sub-beams connected through a massless elastic rotational spring. In the study, the effects of the location of crack, the depth of the crack, foundation stiffness and various material distributions on the natural frequencies and the mode shapes of the cracked functionally graded beams are investigated in detail.

Keywords: Free vibration, Winkler-Pasternak Foundation, Open edge crack, Functionally graded materials,

1. Introduction

Structural elements are subjected to destructive effects in the form of initial defects within the material or caused by fatigue or stress concentration. As a result of destructive effects, cracks occur in the structural elements. It is known that a crack in structure elements introduces a local flexibility, becomes more flexible and its dynamic and static behaviors will be changed. Cracks cause local flexibility and changes in structural stiffness. Therefore, understanding the mechanical behavior and the safe performance of edge-cracked structures is importance in designs.

Functionally graded materials (FGMs) are a new generation of composites where the volume fraction of the FGM constituents vary gradually, giving a non-uniform microstructure with continuously graded macro properties such as elasticity modulus, density, heat conductivity, etc.. Typically, in a FGM, one face of a structural component is ceramic that can resist severe thermal loading and the other face is metal which has excellent structural strength. FGMs consisting of heat-resisting ceramic and fracture-resisting metal can improve the properties of thermal barrier systems because cracking and delamination, which are often observed in conventional layered composites, are reduced by proper smooth transition of material properties. Since the concept of FGMs has been introduced in 1980s, these new kinds of materials have been employed in many engineering application fields, such as aircrafts, space vehicles, defense industries, electronics and biomedical sectors, to eliminate stress concentrations, to relax residual stresses, and to enhance bonding strength. Because of the wide material variations and applications of FGMs, it is important to study the responses of FGM

structures to mechanical and other loadings. With the increased use of FGMs, understanding the mechanical behavior and safe performance of cracked FGM structures is very important.

In the literature, the free vibration and dynamic behavior of homogeneous cracked beams have been extensively studied [1-17]. In recent years, the dynamic behavior of cracked FGM beams has been a topic of active research. Sridhar et al. [18] developed an effective pseudo-spectral finite element method for wave propagation analysis in anisotropic and inhomogeneous structures with or without vertical and horizontal cracks. Briman and Byrd [19] studied the effect of damage on free and forced vibrations of a functionally graded cantilever beam. Yang et al. [20] investigated an analytical study on the free and forced vibration of inhomogeneous Euler–Bernoulli beams containing open edge cracks that the beam is subjected to an axial compressive force and a concentrated transverse load moving along the longitudinal direction. Yang and Chen [21] investigated free vibration and buckling analysis of FGM beams with edge cracks by using Bernoulli–Euler beam theory and the rotational spring model. Free vibration and elastic buckling of beams made of FGM containing open edge cracks are studied within Timoshenko beam theory by Ke et al. [22]. Yu and Chu [23] studied the transverse vibration characteristics of a cracked FGM beam by using the p-version of finite element method. Ke et al. [24] investigated the post-buckling analysis of FGM beams with an open edge crack based on Timoshenko beam theory and von Kármán nonlinear kinematics by using Ritz method. Ferezqi et al. [25] studied an analytical investigation of the free vibrations of a cracked Timoshenko beam made up of FGM. Yan et al. [26] studied dynamic response of FGM beams with an open edge crack resting on an elastic foundation subjected to a transverse load moving at a constant speed. Akbaş [27] investigated static analysis of an edge cracked FGM beam resting on Winkler foundation by using finite element method. Yan et al. [28] investigated the nonlinear flexural dynamic behavior of a clamped Timoshenko beam made of FGM with an open edge crack under an axial parametric excitation which is a combination of a static compressive force and a harmonic excitation force based on Timoshenko beam theory and von Kármán nonlinear kinematics. Wei et al. [29] studied the free vibration of cracked FGM beams with axial loading, rotary inertia and shear deformation by using an analytical method. Akbaş [30,31] studied geometrically nonlinear and post-buckling analysis of edge cracked FG Timoshenko beams. Akbaş [32,33] investigated free vibration and wave propagation of edge cracked FG beams.

In this study is the effect of the parameter of Winkler-Pasternak foundation on natural frequencies and cracks in detail. To obtain more realistic answers and understand to edge cracked FGM beam, more the parameter of FGM property distribution must be used in numerical results. Hence, a lot of the parameters of FGM property distribution are used in this study.

The differential equations of motion are obtained by using Hamilton's principle. The considered problem is investigated within the Euler-Bernoulli beam theory by using finite element method. The cracked beam is modeled as an assembly of two sub-beams connected through a massless elastic rotational spring. Material properties of the beam change in the thickness direction according to exponential distributions. In the study, the effects of the location of crack, the depth of the crack, foundation stiffness and various material distributions on the natural frequencies and the mode shapes of the functionally graded beams are investigated in detail.

2. Theory and Formulations

Consider a cantilever FGM beam of length *L*, width *b*, thickness *h*, containing an edge crack of depth *a* located at a distance L_1 from the left end, resting on Winkler-Pasternak foundation with spring constants k_w and k_p, as shown in Figure 1. It is assumed that the crack is

perpendicular to beam surface and always remains open. When the Pasternak foundation spring constant $k_p = 0$, the foundation model reduces to Winkler type.

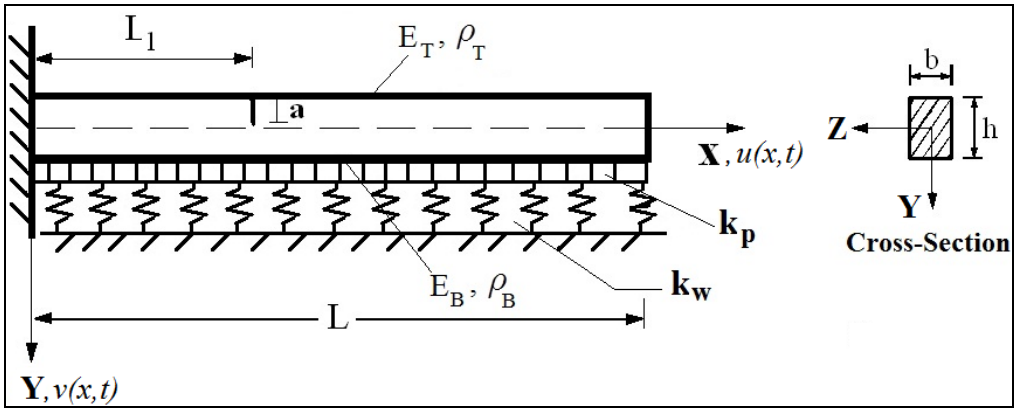

Figure 1: A cantilever FGM beam with an open edge crack resting on Winkler-Pasternak foundation and cross-section.

In this study, Young's modulus $E(Y)$ and mass density $\rho(Y)$ vary continuously in the thickness direction (Y axis) according to exponential distributions as follows;

$$E(Y) = E_0 e^{\beta Y}, \ \rho(Y) = \rho_0 e^{\beta Y} \tag{1}$$

where E_0 and ρ_0 are the Young's modulus and mass density at the midplane (Y=0) of the beam. β is a constant characterizing the gradual variation of the material properties along thickness direction. When $\beta = 0$, the material of the beam is homogeneous. According to Eq. (1) that when $Y = h/2$, $E = E_B$ and $\rho = \rho_B$ (E_B and ρ_B are the Young's modulus and mass density of the bottom). When $Y = -h/2$, $E = E_T$ and $\rho = \rho_T$ (E_T and ρ_T are the Young's modulus and mass density of the top).

According to the coordinate system *(X,Y,Z)* shown in figure 1, based on Euler-Bernoulli beam theory, the axial and the transverse displacement field are expressed as

$$u(X,Y,t) = u_0(X,t) - Y \frac{\partial v_0(X,t)}{\partial X} \tag{2}$$

$$v(X,Y,t) = v_0(X,t) \tag{3}$$

Where u_0 and v_0 are the axial and the transverse displacements in the mid-plane, t indicates time. Using Eq. (2) and (3), the linear strain- displacement relation can be obtained:

$$\varepsilon_{xx} = \frac{\partial u}{\partial X} = \frac{\partial u_0(X,t)}{\partial X} - Y \frac{\partial^2 v_0(X,t)}{\partial X^2} \tag{4}$$

According to Hooke's law, constitutive equations of the FGM beam are as follows:

$$\sigma_{xx} = E(Y)\,\varepsilon_{xx} = E(Y)\left[\frac{\partial u_0(X,t)}{\partial X} - Y \frac{\partial^2 v_0(X,t)}{\partial X^2}\right] \tag{5}$$

Where σ_{xx} and ε_{xx} are normal stresses and normal strains in the X direction, respectively. Based on Euler-Bernoulli beam theory, the elastic strain energy (V) and kinetic energy (T) of the FGM beam resting on Winkler-Pasternak foundation are expressed as

$$V=\frac{1}{2}\int_0^L\int_A \sigma_{xx}\varepsilon_{xx}\,dA\,dX+\frac{1}{2}\int_0^L k_w(v(X,t))^2\,\mathrm{dX}+\frac{1}{2}\int_0^L k_p\left(\frac{\partial v(X,t)}{\partial x}\right)^2\mathrm{dX} \tag{6}$$

$$T=\frac{1}{2}\int_0^L\int_A \rho\ Y\left[\left(\frac{\partial u}{\partial t}\right)^2+\left(\frac{\partial v}{\partial t}\right)^2\right]dA\,dX \tag{7}$$

With applying Hamilton's principle, the differential equations of motion are obtained as follows:

$$A_{XX}\frac{\partial^2 u_0}{\partial X^2}-B_{XX}\frac{\partial}{\partial X}\left(\frac{\partial^2 v_0}{\partial X^2}\right)=I_1\frac{\partial^2 u_0}{\partial t^2}-I_2\frac{\partial^2}{\partial t^2}\left(\frac{\partial v_0}{\partial X}\right) \tag{8}$$

$$B_{XX}\frac{\partial^2}{\partial X^2}\left(\frac{\partial u_0}{\partial X}\right)-D_{XX}\frac{\partial^2}{\partial X^2}\left(\frac{\partial^2 v_0}{\partial X^2}\right)-k_w v_0+k_p\frac{\partial^2 v_0}{\partial X^2}=-I_3\frac{\partial^2}{\partial t^2}\left(\frac{\partial v_0}{\partial X}\right)+I_1\frac{\partial^2 v_0}{\partial t^2} \tag{9}$$

The stiffness components are defined as

$$(A_{XX},B_{XX},D_{XX})=\int_A E(Y)(1,Y,Y^2)dA \tag{10}$$

$$(I_1,I_2,I_3)=\int_A \rho\ Y\ (1,Y,Y^2)dA \tag{11}$$

The displacement field of the finite element shown is expressed in terms of nodal displacements as follows:

$$u_0^{(e)}(X,t)=\varphi_1^{(U)}(X)\ u_1(t)+\varphi_2^{(U)}(X)\ u_2(t) \tag{12}$$

$$v_0^{(e)}(X,t)=\varphi_1^{(V)}(X)v_1(t)+\varphi_2^{(V)}(X)\ \theta_1(t)+\varphi_3^{(V)}(X)\ v_2(t)+\varphi_4^{(V)}(X)\ \theta_2(t) \tag{13}$$

where u_i, v_i and θ_i are axial displacements, transverse displacements and slopes at the two end nodes of the beam element, respectively. $\varphi_i^{(U)}$ and $\varphi_i^{(V)}$ are interpolation functions for axial and transverse degrees of freedom, respectively, which are given in Appendix. Two-node beam element shown in Figure 2.

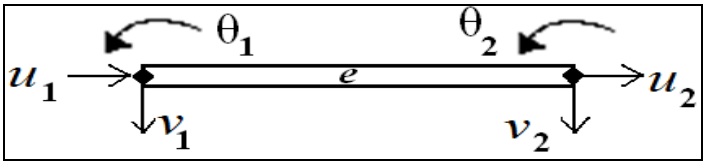

Figure 2: A two-node beam element

With using the standard procedure of the Galerkin finite element method, the stiffness matrix and the mass matrix are obtained according to Eqs. (8) and (9). The equation of motion as follows:

$$\left[K\right]\{q\}+\left[M\right]\{\ddot{q}\}=0 \tag{14}$$

where $\left[K\right]$ is the stiffness matrix and [*M*] is the mass matrix. $\{q\}$ is nodal displacement vector which as follows

$$\{q\}=\{u,v,\theta\}^T \tag{15}$$

The stiffness matrix $\left[K\right]$ can be expressed as a sum of three submatrices as shown below:

$$\left[K\right]=\left[K_b\right]+\left[K_w\right]+\left[K_p\right] \tag{16}$$

Where $\left[K_{(b)}\right]$, $\left[K_{(w)}\right]$ and $\left[K_{(p)}\right]$ are beam stiffness matrix, Winkler foundation stiffness matrix and Pasternak foundation stiffness matrix, respectively. Explicit forms of [*K*] are given in Appendix. The mass matrix $\left[M\right]$ can be expressed as a sum of four sub-matrices as shown below:

$$\left[M\right]=\left[M_U\right]+\left[M_V\right]+\left[M_\theta\right]+\left[M_{U\theta}\right] \tag{17}$$

Where $\left[M_U\right]$, $\left[M_V\right]$ and $\left[M_\theta\right]$ are the contribution of *u*, *v* and θ degree of freedom to the mass matrix, $\left[M_{U\theta}\right]$ is coupling mass matrix due to coupling between *u* and θ. Explicit forms of $\left[M\right]$ are given in Appendix.

The cracked beam is modeled as an assembly of two sub-beams connected through a massless elastic rotational spring shown in figure 3.

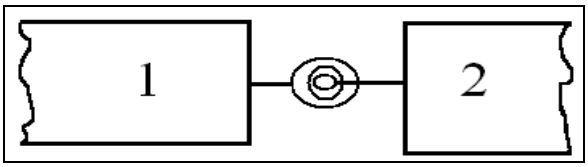

Figure 3. Rotational spring model.

The bending stiffness of the cracked section k_T is related to the flexibility G by

$$k_T=\frac{1}{G} \tag{18}$$

Cracked section's flexibility G can be derived from Broek's approximation [34]:

$$\frac{(1-\nu^2)K_I^2}{E(a)}=\frac{M^2}{2}\frac{\mathrm{dG}}{\mathrm{da}} \tag{19}$$

where M is the bending moment at the cracked section, K_I is the stress intensity factor (SIF) under mode I bending load and is a function of the geometry, the loading, and the material properties as well. ν indicates Poisson's ratio which is taken to be constant since its influence on the stress intensity factors is quite limited [35]. For an FGM strip with an open edge crack under bending, the analytical solution and the expression of SIF is given Yu And Chu [23] that obtained from the data given by Erdogan and Wu [35] through Lagrange interpolation technique:

$$K_I = \frac{6M}{bh^2}\sqrt{\pi a}\,F(E_R, a/h) \tag{20}$$

Where a is depth of crack, E_R is the ratio of Young's modulus of bottom and top surfaces of the beam (E_B/E_T) and F is an unknown function of two independent variables. The function F is can be expressed as follows [23];

$$F(E_R, a/h) = \frac{p_1 + p_2\ln(E_R) + p_3[\ln(E_R)]^2 + p_4[\ln(E_R)]^3 + p_5(a/h) + p_6(a/h)^2}{1 + p_7\ln(E_R) + p_8[\ln(E_R)]^2 + p_9(a/h) + p_{10}(a/h)^2 + p_{11}(a/h)^3} \tag{21}$$

Where the coefficients $p_1, p_2, \ldots, p_{10}, p_{11}$ =1.1732, -0.3539, 0.0289, -0.0061, 0.6625, 3.072, -0.0014, -0.0017, 1.9917, -0.3496, -3.0982 are given in Yu And Chu [23] that are determined by fitting Eq. (20) based on the least square method to the numerical values of the SIF for specific material gradients and normalized crack size given by Erdogan and Wu [35].

The spring connects the adjacent left and right elements and couples the slopes of the two FGM beam elements at the crack location. In the massless spring model, the compatibility conditions enforce the continuities of the axial displacement, transverse deflection, axial force and bending moment across the crack at the cracked section ($X = L_1$), that is,

$$u_1 = u_2,\ v_1 = v_2,\ N_1 = N_2, M_1 = M_2 \tag{22}$$

The discontinuity in the slope is as follows:

$$k_T\left(\frac{dv_1}{dX} - \frac{dv_2}{dX}\right) = k_T(\theta_1 - \theta_2) = M_1 \tag{23}$$

Based on the massless spring model, the stiffness matrix of the cracked section as follows:

$$[K]_{Cr} = \begin{bmatrix} 1/G & -1/G \\ -1/G & 1/G \end{bmatrix} = \begin{bmatrix} k_T & -k_T \\ -k_T & k_T \end{bmatrix} \tag{24}$$

The stiffness matrix of the cracked section is written according to the displacement vector:

$$\{q\}_{(Cr)} = \{\theta_1, \theta_2\}^T \tag{25}$$

Where θ_1 and θ_2 are the angles of the cracked section. With adding crack model, the equations of motion for the finite element and by use of usual assemblage procedure the following system of equations of motion for the whole system can be obtained as follows:

$$(\left[K\right] + \left[K\right]_{(Cr)})\{q\} + \left[M\right]\{\ddot{q}\} = 0 \tag{26}$$

If the global nodal displacement vector $\{q\}$ is assumed to be harmonic in time with circular frequency ω, i.e $\{q\} = \{\bar{q}\}e^{i\omega t}$ becomes, after imposing the appropriate end conditions, an eigenvalue problem of the form:

$$(\left[K\right] + \left[K\right]_{(Cr)} - \omega^2\left[M\right])\{\bar{q}\} = 0 \tag{27}$$

Where $\{\hat{q}\}$ is a vector of displacement amplitudes of the vibration. The dimensionless quantities can be expressed as

$$\bar{\omega}=\frac{\omega L^2}{\sqrt{D_0/I_{10}}},\ \bar{k}_w=\frac{k_w L^4}{D_0},\ \bar{k}_p=\frac{k_p L^2}{D_0},\ \bar{X}=\frac{X}{L},\ \bar{Y}=\frac{Y}{h},\ E_R=\frac{E_B}{E_T},\ \rho_R=\frac{\rho_B}{\rho_T} \quad (28)$$

Where $\bar{\omega}$ is the dimensionless frequency, $\bar{k}_w$ is the dimensionless Winkler parameter, $\bar{k}_p$ is the dimensionless Pasternak parameter, E_R is the ratio of Young's modulus of bottom and top surfaces of the beam, ρ_R is the ratio of mass density of bottom and top surfaces of the beam. D_0 and I_{10} indicate the value of D_{XX} and I_1 of an isotropic homogeneous beam.

3. Numerical Results

In the numerical examples, the natural frequencies and the mode shapes of the beams are calculated and presented in figures for various the effects of the location of crack, the depth of the crack, foundation stiffness and material distributions. The beam considered in numerical examples is made of Aluminum ($E=70GPa$, $\nu=0.33$, $\rho=2780\,kg/m^3$) which the material constants change exponentially as in Eq. (1). The top surface of the FGM beam is Aluminum. In the numerical integrations, five-point Gauss integration rule is used. Unless otherwise stated, it is assumed that the width of the beam is $b=0.1m$, height of the beam is $h=0.1m$ and length of the beam is $L=30h$ in the numerical results. In the numerical calculations, the number of finite elements is taken as *n* = 100.

In figure 4, the effect of the dimensionless Winkler parameter $\bar{k}_w$ on the dimensionless fundamental frequency $\bar{\omega}_1$ of edge cracked FGM beams ($E_R=2$, $a/h=0.6$, $\bar{k}_p=0$) are shown for various the crack location L_1/L.

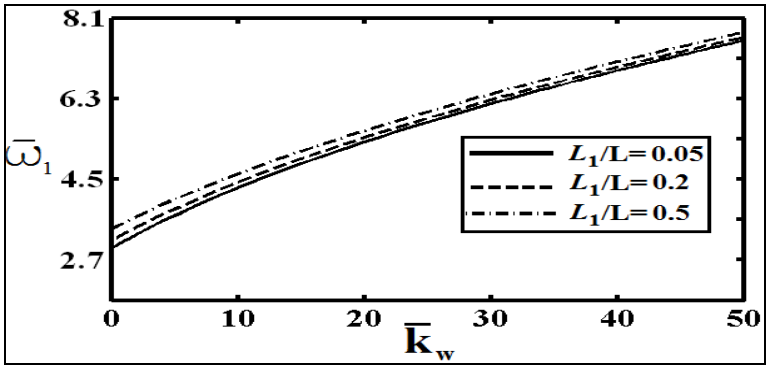

Figure 4: The effect the dimensionless Winkler parameter $\bar{k}_w$ on the dimensionless fundamental frequency $\bar{\omega}_1$ for various the crack location L_1/L.

It is seen from figure 4 that the increasing the value of the dimensionless Winkler parameter $\bar{k}_w$ play important role on the fundamental frequency. With increase in the dimensionless Winkler parameter $\bar{k}_w$, the fundamental frequency increases. Because, with increasing the Winkler parameter $\bar{k}_w$, the beam gets more stiffer. Also, it is observed figure 4 that the

differences between of the crack location L_1/L decrease with increase the Winkler parameter $\bar{k}_w$.

Figure 5 shows that the effect of the dimensionless Winkler parameter $\bar{k}_w$ on the dimensionless fundamental frequency $\bar{\omega}_1$ of edge cracked FGM beams ($E_R=2$, $L_1/L=0.05$, $\bar{k}_p=0$) are shown for various the crack depth ratio a/h.

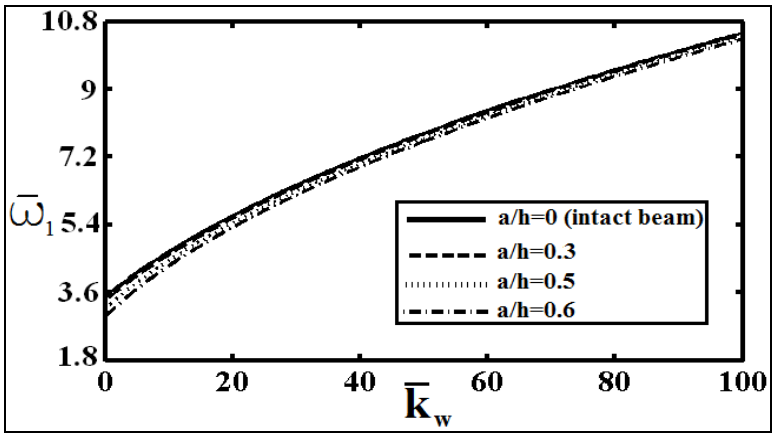

Figure 5: The effect the dimensionless Winkler parameter $\bar{k}_w$ on the dimensionless fundamental frequency $\bar{\omega}_1$ for various the crack depth ratio a/h.

It is seen from figure 5 that with the increasing the value of the dimensionless Winkler parameter $\bar{k}_w$, the differences between of the crack depth ratio a/h decrease. Increases with the stiffness parameter of the foundation, the effects of the crack reduce.

In Figure 6, the effect of the the dimensionless Winkler parameter $\bar{k}_w$ on the dimensionless fundamental frequency $\bar{\omega}_1$ of edge cracked FGM beams ($a/h=0.6$, $L_1/L=0.05$, $\bar{k}_p=0$) are shown for $E_R=2$ and $E_R=0.5$.

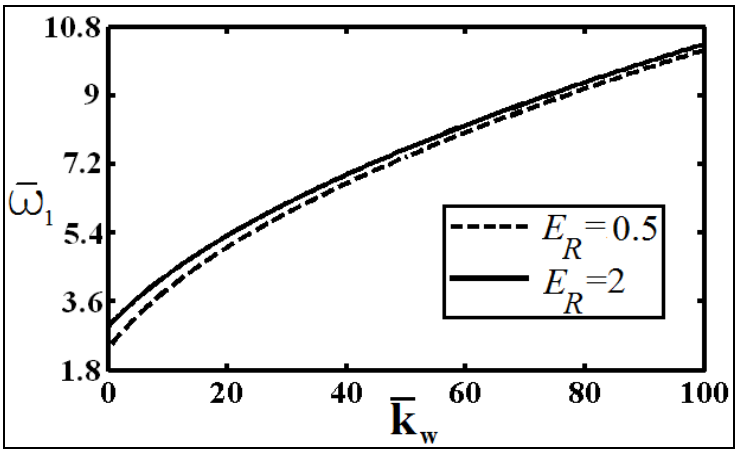

Figure 6: The effect the dimensionless Winkler parameter $\bar{k}_w$ on the dimensionless fundamental frequency $\bar{\omega}_1$ for $E_R=2$ and $E_R=0.5$.

It is seen from figure 6 that with increase in the value of the dimensionless Winkler parameter $\bar{k}_w$, the difference between the dimensionless fundamental frequency of $E_R = 2$ and $E_R = 0.5$ decreases. It is shown results that the stiffness parameter of the foundation is very effective for reducing disadvantage of cracks.

Figure 7 displays the effect of the dimensionless Winkler parameter $\bar{k}_w$ on the first and second normalized vibration mode shapes for $E_R = 2$, $L_1/L = 0.05$, $a/h = 0.6$, $\bar{k}_p = 0$.

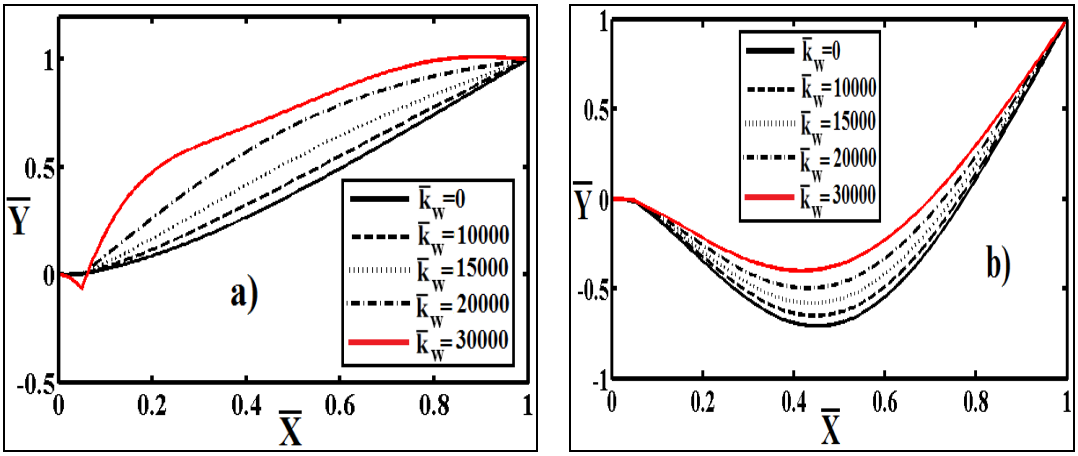

Figure 7: The effect the dimensionless Winkler parameter $\bar{k}_w$ on the a) first and b) second normalized vibration mode shapes.

It is seen from figure 7 that with increase in the value of dimensionless Winkler parameter $\bar{k}_w$, vibration mode shapes change significantly. It is observed from the results, the stiffness parameter of the foundation is very effective for the mechanical behavior of the beam. It is observed from figure 7 that the dimensionless Winkler parameter $\bar{k}_w$ is more effective in first vibration mode than second vibration mode.

In figure 8, the effect of the dimensionless Pasternak parameter $\bar{k}_p$ on the dimensionless fundamental frequency $\bar{\omega}_1$ of edge cracked FGM beams ($E_R = 2$, $a/h = 0.6$, $\bar{k}_w = 10$) are shown for various the crack location L_1/L.

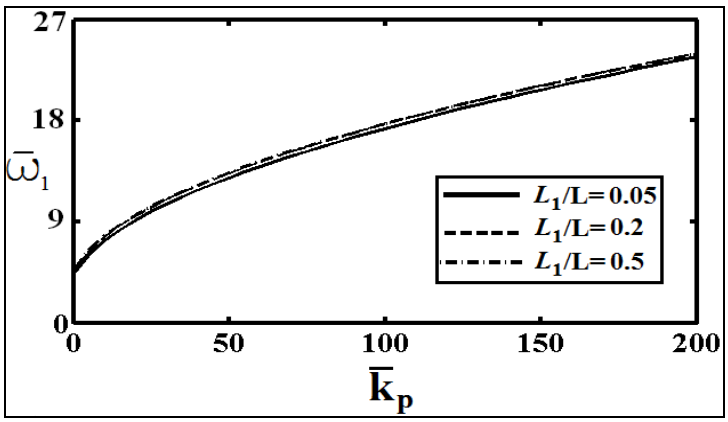

Figure 8: The effect the dimensionless Pasternak parameter $\bar{k}_p$ on the dimensionless fundamental frequency $\bar{\omega}_1$ for various the crack location L_1/L.

It is seen from figure 8 that with increase in the dimensionless Pasternak parameter $\bar{k}_p$, the fundamental frequency increases. Because, with increasing the Pasternak parameter $\bar{k}_p$, the beam gets more stiffer. The effect of Pasternak parameter $\bar{k}_p$ on the dimensionless fundamental frequency is less than Winkler parameter $\bar{k}_w$ for various the crack location L_1/L.

Figure 9 shows that the effect of the dimensionless Pasternak parameter $\bar{k}_p$ on the dimensionless fundamental frequency $\bar{\omega}_1$ of edge cracked FGM beams ($E_R = 2$, $L_1/L = 0.05$, $\bar{k}_w = 10$) are shown for various the crack depth ratio a/h. In figure 10, the effect of the the dimensionless Pasternak parameter $\bar{k}_p$ on the dimensionless fundamental frequency $\bar{\omega}_1$ of edge cracked FGM beams ($a/h = 0.6$, $L_1/L = 0.05$, $\bar{k}_w = 10$) are shown for $E_R = 2$ and $E_R = 0.5$.

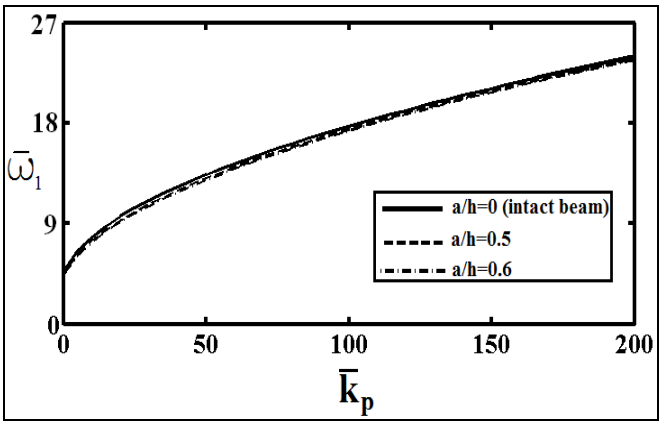

Figure 9: The effect the dimensionless Pasternak parameter $\bar{k}_p$ on the dimensionless fundamental frequency $\bar{\omega}_1$ for various the crack depth ratio a/h.

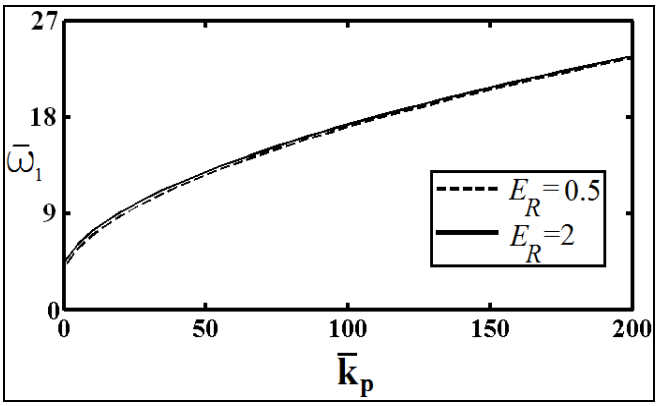

Figure 10: The effect the dimensionless Pasternak parameter $\bar{k}_p$ on the dimensionless fundamental frequency $\bar{\omega}_1$ for $E_R = 2$ and $E_R = 0.5$.

It is seen from figure 9 and figure 10 that the stiffness parameter of the Pasternak foundation is not effective for reducing disadvantage of cracks, significantly.

Figure 11 displays the effect of the dimensionless Pasternak parameter $\bar{k}_p$ on the first and second normalized vibration mode shapes for $E_R = 2$, $L_1/L = 0.05$, $a/h = 0.6$, $\bar{k}_w = 10$.

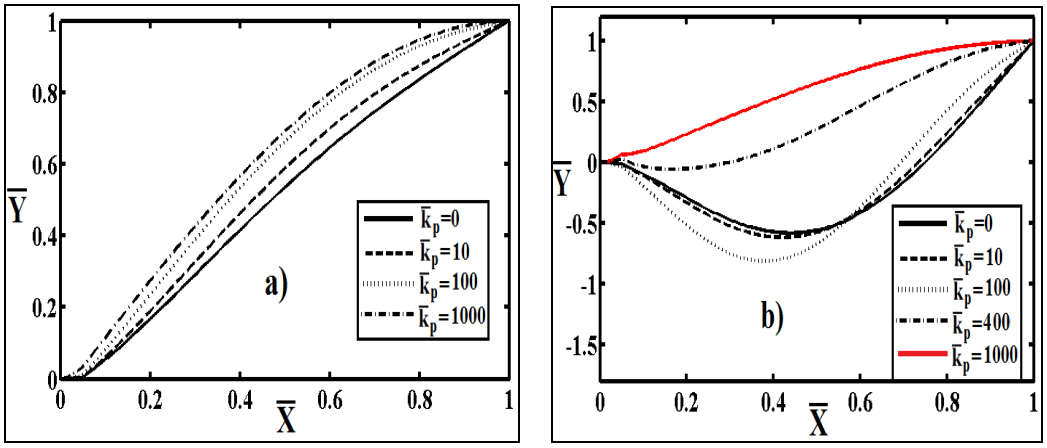

Figure 11: The effect the dimensionless Pasternak parameter $\bar{k}_p$ on the a) first and b) second normalized vibration mode shapes.

It is seen from figure 11 that with increase in the value of dimensionless Pasternak parameter $\bar{k}_p$, vibration mode shapes change significantly. It is observed from figure 11 that the dimensionless Pasternak parameter $\bar{k}_p$ is more effective in second vibration mode than first vibration mode.

4. Conclusions

Free vibration analysis of an edge cracked FGM cantilever beam resting on Winkler-Pasternak foundation are investigated within the Euler-Bernoulli beam theory by using finite element method. Material properties of the beam change in the thickness direction according to an exponential function. The differential equations of motion are obtained by using Hamilton's principle. The cracked beam is modeled as an assembly of two sub-beams connected through a massless elastic rotational spring. The influences of the location of crack, the depth of the crack, foundation stiffness and various material distributions on the natural frequencies and the mode shapes of the FGM beams are examined in detail.
The following conclusions are reached from the obtained results:

(1) The crack locations and the crack depth have a great influence on the vibration characteristics of the FGM beam.

(2) The stiffness parameter of Winkler foundation is very effective for reducing disadvantage of cracks.

(3) The stiffness parameter of the Pasternak foundation is not effective for reducing disadvantage of cracks.

(4) The stiffness parameters of the foundation have a great influence on vibration mode shapes.

Appendix

The interpolation functions for axial degrees of freedom are

$$\varphi^{(U)}(X)=\left[\varphi_1^{(U)}(X)\ \ \varphi_2^{(U)}(X)\right]^T, \tag{A1}$$

where

$$\varphi_1^{(U)}(X)=\left(-\frac{X}{L_e}+1\right), \tag{A2}$$

$$\varphi_2^{(U)}(X)=\left(\frac{X}{L_e}\right), \tag{A3}$$

The interpolation functions for transverse degrees of freedom are

$$\varphi^{(V)}(X)=\left[\varphi_1^{(V)}(X)\ \ \varphi_2^{(V)}(X)\ \ \varphi_3^{(V)}(X)\ \ \varphi_4^{(V)}(X)\right]^T, \tag{A4}$$

where

$$\varphi_1^{(V)}(X)=\left(1-\frac{3X^2}{L_e^2}+\frac{2X^3}{L_e^3}\right), \tag{A5}$$

$$\varphi_2^{(V)}(X)=\left(-X+\frac{2X^2}{L_e}-\frac{X^3}{L_e^3}\right), \tag{A6}$$

$$\varphi_3^{(V)}(X)=\left(\frac{3X^2}{L_e^2}-\frac{2X^3}{L_e^3}\right), \tag{A7}$$

$$\varphi_4^{(V)}(X)=\left(\frac{X^2}{L_e}-\frac{X^3}{L_e^3}\right), \tag{A8}$$

where L_e indicates the length of the finite beam element. The components of the stiffness matrix $\left[K\right]$: the beam stiffness matrix $\left[K_b\right]$, Winkler foundation stiffness matrix $\left[K_w\right]$ and Pasternak foundation stiffness matrix $\left[K_p\right]$ are as follows

$$\left[K_b\right]=\begin{bmatrix}\left[K_{(b)}^A\right] & \left[K_{(b)}^B\right]\\ \left[K_{(b)}^B\right]^T & \left[K_{(b)}^D\right]\end{bmatrix}, \tag{A9}$$

where

$$\left[K_{(b)}^A\right]=\int_0^{L_e} A_{XX}\left[\frac{d\varphi^{(U)}}{dX}\right]^T\left[\frac{d\varphi^{(U)}}{dX}\right]dX, \tag{A10}$$

$$\left[K_{(b)}^B\right]=-\int_0^{L_e} B_{XX}\left[\frac{d^2\varphi^{(V)}}{dX^2}\right]^T\left[\frac{d\varphi^{(U)}}{dX}\right]dX \tag{A11}$$

$$\left[K_{(b)}^D\right]=\int_0^{L_e} D_{XX}\left[\frac{d^2\varphi^{(V)}}{dX^2}\right]^T\left[\frac{d^2\varphi^{(V)}}{dX^2}\right]dX, \tag{A12}$$

$$\left[K_w\right]=\int_0^{L_e} k_w\left[\varphi^{(V)}\right]^T\left[\varphi^{(V)}\right]dX\,, \tag{A13}$$

$$\left[K_p\right]=\int_0^{L_e} k_p\left[\frac{d\varphi^{(V)}}{dX}\right]^T\left[\frac{d\varphi^{(V)}}{dX}\right]dX\,, \tag{A14}$$

The components of the mass matrix $\left[M\right]$: $\left[M_U\right]$, $\left[M_V\right]$, $\left[M_\theta\right]$ and $\left[M_{U\theta}\right]$ are as follows

$$\left[M_U\right]=\int_0^{L_e} I_1\left[\varphi^{(U)}\right]^T\left[\varphi^{(U)}\right]dX \tag{A15}$$

$$\left[M_V\right]=\int_0^{L_e} I_1\left[\varphi^{(V)}\right]^T\left[\varphi^{(V)}\right]dX \tag{A16}$$

$$\left[M_\theta\right]=\int_0^{L_e} I_3\left[\frac{d\varphi^{(V)}}{dX}\right]^T\left[\frac{d\varphi^{(V)}}{dX}\right]dX \tag{A17}$$

$$\left[M_{U\theta}\right]=-\int_0^{L_e} I_2\left(\left[\varphi^{(U)}\right]^T\left[\frac{d\varphi^{(V)}}{dX}\right]+\left[\frac{d\varphi^{(V)}}{dX}\right]^T\left[\varphi^{(U)}\right]\right)dX \tag{A18}$$

References

[1] Dimarogonas, A.D., Vibration of Cracked Structures: A State of the Art Review. *Engineering Fracture Mechanics*, 55, 831–857, 1996.

[2] Yokoyama, T. and Chen, M.C., Vibration Analysis of Edge-Cracked Beams using a Line-Spring Model. *Engineering Fracture Mechanics*,59, 403–409,1998.

[3] Kisa, M., Brandon, J. and Topcu, M. Free Vibration Analysis of Cracked Beams by a Combination of Finite Elements and Component Mode Synthesis Methods. *Computers and Structures*, 67, 215–223, 1998.

[4] Chondros, T.G., Dimarogonas, A.D. and Yao, J., A continuous cracked beam vibration Theory. *Journal of Sound and Vibration*, 215, 17–34, 1998.

[5] Kısa, M. and Brandon, J.A. "Free vibration analysis of multiple openedge cracked beams by component mode synthesis," *Structural Engineering Mechanics*,10, 81-92, 2000.

[6] Lin, H.P., Chang, S.C. and Wu, J.D., Beam vibrations with an arbitrary number of Cracks. *Journal of Sound and Vibration*, 258, 987–999, 2002.

[7] Nag, A., Roy Mahapatra, D., Gopalakrishnan, S. and Sankar, T.S., A Spectral Finite Element with Embedded Delamination for Modeling of Wave Scattering in Composite Beams. *Composites Science and Technology*, 63, 2187–2200, 2003.

[8] Zheng, D.Y. and Kessissoglou, N.J., Free vibration analysis of a cracked beam by finite element method. *Journal of Sound and Vibration*, 273, 457–475, 2004.

[9] Kısa, M., Free Vibration analysis of a cantilever composite beam with multiple cracks. *Composites Science and Technology*, 64, 1391-1402, 2004.

[10] El Bikri, K., Benamar, R. and Bennouna, M.M.,Geometrically Non-Linear Free Vibrations of Clamped-Clamped Beams with an Edge Crack. *Computers & Structures*, 84, 485–502, 2006.

[11] Kısa, M. and Gürel, M.A., Free vibration analysis of uniform and stepped cracked beams with circular cross sections. *International Journal of Engineering Science*, 45, 364–380, 2007.

[12] Aydin, K., Vibratory characteristics of Euler-Bernoulli beams with an arbitrary number of cracks subjected to axial load. *Journal of Vibration and Control*, 14, 485-510, 2008.

[13] Shafiei, M. and Khaji, N., Analytical solutions for free and forced vibrations of a multiple cracked Timoshenko beam subject to a concentrated moving load. *Acta Mechanica*, 221, 79–97, 2011.
[14] Akbaş, Ş.D., Free vibration characteristics of edge cracked piles with circular cross section. *International Journal of Engineering Research and Applications*, 3, 363-371, 2013.
[15] Akbaş, Ş.D., Wave propagation analysis of edge cracked beams resting on elastic foundation. *International Journal of Engineering and Applied Sciences*, 6,40- 52, 2014.
[16] Akbaş, Ş.D., Wave Propagation Analysis of Edge Cracked Circular Beams under Impact Force. *PLos One*, 9(6), 100496, 2014.
[17] Akbaş, Ş.D., Large Deflection Analysis of Edge Cracked Simple Supported Beams. *Structural Engineering and Mechanics*, 54, 433-451, 2015.
[18] Sridhar, R., Chakraborty, A. and Gopalakrishnan, S., Wave Propagation Analysis in Anisotropic and Inhomogeneous Uncracked and Cracked Structures using Pseudospectral Finite Element Method. *International Journal of Solids and Structures*, 43, 4997–5031, 2006.
[19] Briman, V. and Byrd, L.W., Vibration of Damaged Cantilevered Beams Manufactured from Functionally Graded Materials. *AIAA Journal*., 45, 2747–2757, 2007.
[20] Yang, J., Chen, Y., Xiang, Y. and Jia, X.L., Free and Forced Vibration of Cracked Inhomogeneous Beams under an Axial Force and a Moving Load," *Journal of Sound and Vibration*, 312, 166–181, 2008.
[21] Yang, J. and Chen, Y., Free Vibration and Buckling Analyses of Functionally Graded Beams with Edge Cracks. *Composite Structures*, 83, 48–60, 2008.
[22] Ke, L. L., Yang, J., Kitipornchai, S. and Xiang,Y., Flexural Vibration and Elastic Buckling of a Cracked Timoshenko Beam Made of Functionally Graded Materials. *Mechanics of Advanced Materials and Structures*,16, 488–502, 2009.
[23] Yu, Z. and Chu, F., Identification of crack in functionally graded material beams using the *p*- version of finite element method, *Journal of Sound and Vibration*, 325, 69–84, 2009.
[24] Ke, L. L., Yang, J. and Kitipornchai, S., Postbuckling analysis of edge cracked functionally graded Timoshenko beams under end shortening. *Composite Structures*, 90, 152–160, 2009.
[25] Ferezqi, H.Z., Tahani, M. and Toussi, H.E., Analytical approach to free vibrations of cracked Timoshenko beams made of functionally graded materials. *Mechanics of Advanced Materials and Structures*,17, 353–65, 2010.
[26] Yan, T., Kitipornchai, S., Yang, J. and He, X. Q., Dynamic behaviour of edge-cracked shear deformable functionally graded beams on an elastic foundation under a moving load. *Composite Structures*, 93, 2992–3001, 2011.
[27] Akbaş, Ş.D., Static analysis of a functionally graded beam with edge cracks on elastic foundation, *Proceedings of the 9 th International Fracture Conference*, Istanbul, Turkey, 2011.
[28] Yan, T., Yang, J. and Kitipornchai, S., Nonlinear dynamic response of an edge-cracked functionally graded Timoshenko beam under parametric excitation. *Nonlinear Dynamics*, 67, 527–540, 2012.
[29] Wei, D., Liu, Y. and Xiang, Z., An analytical method for free vibration analysis of functionally graded beams with edge cracks. *Journal of Sound and Vibration*, 331, 1686–1700, 2012.
[30] Akbaş, Ş.D., Geometrically Nonlinear Static Analysis of Edge Cracked Timoshenko Beams Composed of Functionally Graded Material. Mathematical Problems in Engineering, 2013, Article ID 871815, 14 pages, 2013.

[31] Akbaş, Ş.D., Free vibration characteristics of edge cracked functionally graded beams by using finite element method. *International Journal of Engineering Trends and Technology*, 4, 4590-4597, 2013.
[32] Akbaş, Ş.D. Wave Propagation in Edge Cracked Functionally Graded Beams Under Impact Force. *Journal of Vibration and Control*, 1-15, Doi: 10.1177/1077546314547531, 2014.
[33] Akbaş, Ş.D., On Post-Buckling Behavior of Edge Cracked Functionally Graded Beams Under Axial Loads. *International Journal of Structural Stability and Dynamics*, 15, 1450065, 2015.
[34] D. Broek, *Elementary engineering fracture mechanics*, Martinus Nijhoff Publishers, Dordrecht, 1986.
[35] F. Erdogan and B.H. Wu, "The Surface Crack Problem for a Plate with Functionally Graded Properties," *Journal of Applied Mechanics*, vol. 64, no. 3, pp. 448–456, 1997.